Eur. Phys. J. A **25**, s01, 633–638 (2005)
DOI: 10.1140/epjad/i2005-06-157-2

EPJ A direct
electronic only

r-process isotopes in the ^{132}Sn region

K.-L. Kratz[1,2,3,a], B. Pfeiffer[1,2], O. Arndt[1], S. Hennrich[1,2], A. Wöhr[3,4], and the ISOLDE/IS333, IS378, IS393 Collaborations

[1] Institut für Kernchemie, Universität Mainz, D-55128 Mainz, Germany
[2] Virtual Institute for Nuclear Structure and Astrophysics, Germany[b]
[3] Department of Physics, University of Notre Dame, Notre Dame, IN 46556, USA
[4] Joint Institute for Nuclear Astrophysics, USA[c]

Received: 17 January 2005 /
Published online: 18 July 2005 –

Abstract. A correct understanding of r-process nucleosynthesis requires the knowledge of nuclear-structure properties far from β-stability and a detailed description of the possible astrophysical environments. With respect to nuclear data, in recent years the main focus at CERN/ISOLDE has been put on the ^{132}Sn region to explore the role of the $N = 82$ shell closure and its consequences on the r-process matter flow through the $A \simeq 130$ Solar-System r-abundance peak.

PACS. 26.30.+k Nucleosynthesis in novae, supernovae and other explosive environments – 26.50.+x Nuclear physics aspects of novae, supernovae, and other explosive environments – 27.60.+j $90 \leq A \leq 149$ – 97.60.Bw Supernovae

1 Introduction

Nucleosynthesis theory predicts that neutron-capture processes are responsible for the formation of the predominant part of elements heavier than Fe (for historical reviews, see *e.g.* [1,2,3]). The Solar-System abundance pattern ($N_\odot$) of heavy nuclei, in particular the splitting of the $N_\odot$ peaks (see, *e.g.*, fig. 1 in ref. [1]), reveals evidence for two distinct neutron-capture processes in nature —one at low neutron densities ($n_n \simeq 10^8$ cm^{-3}) and the other at high neutron densities ($n_n \geq 10^{20}$ cm^{-3}). Historically, this has led to the definition of the *s-process* (slow neutron capture) and the *r-process* (rapid neutron capture) which are identified with different astrophysical environments.

Besides this basic understanding, the history of r-process research has been quite diverse in suggested astrophysical scenarios (for reviews, see, *e.g.*, [4,5,6,7]). In any case, the observation of the three r-process abundance ($N_{r,\odot}$) peaks at $A \simeq 80$, 130 and 195, which are correlated with the neutron shell closures at $N = 50$, 82 and 126 far from β-stability, suggests that the operation of such a nucleosynthesis process requires conditions that can only be provided by explosive scenarios. Although the question of the exact r-process site(s) is still an open one, type-II supernovae (SNII) and neutron star mergers (NSM; or similar events) are suggested most frequently today.

[a] Conference presenter; e-mail: klkratz@uni-mainz.de
[b] http://www.vistars.de
[c] http://www.jina-web.org

2 Nuclear-physics needs for r-process calculations

The necessary high neutron-density (n_n) and temperature ($T_9 = 10^9$ K) environments result in local mass regions with quasi-statistical equilibria (QSE), where the (n,$\gamma \rightleftharpoons \gamma$,n) equilibrium balance is set by nuclear masses (*i.e.* the neutron separation energies (S_n)). For a given n_n-T_9 condition, the r-process then proceeds along a *"contour line"* of constant S_n to heavier-Z nuclei (see, *e.g.* fig. 4 in [8]). The weak interactions connecting the elements are the β-decays at the *"waiting points"*, which act as bottle necks for the r-process matter flow. Thus, when assuming an additional β-flow equilibrium, in principle the knowledge of nuclear masses (S_n values) and β-decay half-lives ($T_{1/2}$) would be sufficient to determine the whole set of the initial (progenitor) r-process abundances prior to the decay back to stability. This then implies approximate equality of progenitor abundance ($N_{r,prog}$) times β-decay rate ($\lambda_\beta = \ln 2/T_{1/2}$). Thus, with $N_{r,prog}(Z)\lambda_\beta(Z) \simeq$ const the $T_{1/2}$ along the r-process flow path would in turn define the $N_{r,prog}$, and —when taking into account delayed neutron emission (P_n branching) during freeze-out— also the final $N_{r,\odot}$. A verification of the validity of this simple and elegant approximation requires, however, *experimental* information on far-unstable waiting-point isotopes, for a long time believed to be inaccessible in terrestrial laboratories. However, with the identification of the first two classical neutron-magic waiting-point isotopes, $N = 82$ ^{130}Cd at

CERN/ISOLDE [9], and $N = 50$ ^{80}Zn at OSIRIS [10] and TRISTAN [11], Kratz *et al.* [9,12,13] could show first evidence for the existence of local steady-flow equilibria. This result immediately presented a stimulating challenge to both theoreticians and experimentalists in the nuclear-astrophysics community in the following years. Today, about 35 r-process isotopes have been identified via at least a β-decay half-life determination (see, *e.g.* [14,15]).

Nevertheless, the vast majority of r-process nuclei is still experimentally not accessible. Therefore, their nuclear properties can only be obtained through theoretical means. Since a number of different quantities are needed in r-process calculations, as outlined above, in the past it was often not possible to derive them all from one source. Taking them from different sources, however, in particular from models with largely different sophistication, may raise the question of consistency. Therefore, since more than a decade our collaboration has performed various r-process calculations in a unified macroscopic-microscopic approach in which all nuclear properties can be studied in an internally consistent way. This approach is, for example, discussed in detail in [13,16] for the combination of nuclear masses from the Finite Range Droplet Model (FRDM; [17]) and gross β-decay properties ($T_{1/2}$ and P_n values) from a Quasi-Particle Random Phase Approximation (QRPA) of Gamow-Teller (GT) transitions. In its present version, the model also includes first-forbidden (ff) corrections [18]. Analoguously, when adopting other mass formulae, such as the Extended Thomas-Fermi plus Strutinsky Integral (ETFSI) models (see, *e.g.*, [19]), or the more recent Skyrme Hartree-Fock-Bogolyubov (HFB) models of the Montreal-Brussels group (see, *e.g.*, [20,21]), we normally use theoretical β-decay quantities deduced from QRPA calculations with masses and deformation parameters given by that particular model.

It has been claimed by different authors, that mass models as well as theoretical approaches to calculate β-decay that go beyond the single-particle (SP) ansatz would by virtue of their added microscopic complexity be physically more reliable than gross-theory and macroscopic-microscopic models, and would provide better predictive power for unknown nuclei. However, recent tests of various HF mean-field and large-scale shell models clearly show that these expectations have so far not been fulfilled (see, *e.g.* [15,22,23,24,25]).

As far as nuclear masses are concerned, none of the ETFSI, HF-BCS or the recent HFB model versions of the Montreal-Brussels group exhibit the reliability of the FRDM predictions from 1992 for the recent substantially expanded experimental data base of NUBASE [26]. Moreover, there seem to be fundamental problems with the HFB models. Several parameters are clearly not treated in a *"self-consistent"* and *"fully microsocopic"* way [22,24]. In any case, it is somehow worrying to see the number of parameters to optimize the global mass fits in these approaches increasing from about 10 for the earlier ETFSI models to 20 for HFB-8 when practically no improvement of the quality of fits to known masses is achieved. This is most evident in the mass regions relevant to r-process calculations, in particular the far-unstable regions of the neutron shell closures (see, *e.g.*, [15] for further discussion). In the most recent HFB mass model, HFB-9 [27], where (in contrast to the earlier HFB versions) the nuclear-matter symmetry coefficient has been fixed to $J = 30$ MeV, the rms deviation of the fit to the data from NUBASE [26] has even *increased* again from 0.635 to 0.733 MeV. For comparison, the rms deviation of the "old" macroscopic-microscopic FRDM, which was adjusted to the masses known in 1989, is 0.616 MeV [28].

Over the years, various theoretical approaches have been developed to model β-decay (for a recent review, see, *e.g.*, [25]). As in the case of nuclear masses, these approaches have largely different applicability and sophistication. Some models emphasise global applicability, whereas others seek selfconsistency or the comprehensive inclusion of nuclear correlations. Unfortunately, to date none of these models contains all important aspects in a consistent way. Even the most recent "microscopic" models have strong limitations in that they are restricted either to GT-transitions, to spherical shapes and/or to even-even nuclei (see, *e.g.*, [15,25,29]), or use a too small SP modelspace [30,31]. Moreover, the information made available in order to judge the physical reliability of these approaches to calculate gross β-decay properties is often very limited. Therefore, for the time being these models are unsuitable as a basis for global dynamical r-process calculations. As mentioned already above, there is so far only one largely consistent approach with global applicability capable of predicting a variety of nuclear properties, namely the latest FRDM+QRPA version [18]. This model shows an average error in predicting $T_{1/2}$ far from stability of about 3. Accordingly, the average error for P_n values is 3.5 (see, *e.g.*, figs. 4 and 5 in [18]). Progress in the above approaches certainly asks for more than just the reproduction of known gross β-decay properties, but for a detailed prediction of the full *"β-strength distribution"*, which has to be deduced from quantities such as the Q_β value, the main GT- and low-lying ff-transitions and their $\log(ft)$ values. It is somehow worrying to see that several recent microscopic models succeed to reproduce the measured $T_{1/2}$ of the $N = 82$ waiting-point isotope ^{130}Cd, but either on the basis of an incorrect input of (part of) the above mentioned quantities [30,31], or with the simultaneous result of a *stable* double-magic ^{132}Sn nucleus (with $T_{1/2}(\mathrm{exp}) = 40$ s) just one proton pair above ^{130}Cd [29]. This implies that in this relativistic PN-RQRPA model the isobaric mass difference between ^{132}Sn and ^{132}Sb is too low by at least the known Q_β value of 3.12 MeV [26].

3 Experimental information on r-process nuclei

The experimental study of neutron-rich nuclides lying in and near the projected r-process boulevard serves two purposes, i) provision of direct data for use in nucleosynthesis calculations, in particular at magic neutron shells, and ii) testing the theories from which

Table 1. Comparison of experimental half-lives ($T_{1/2}$) with a recent update of the empirical Kratz-Herrmann formula (KHF) and different shell-model predictions for pure Gamow-Teller (GT) and GT plus first-forbidden (GT+ff) decays.

Isotope	Beta-decay half-life, $T_{1/2}$ (ms)						
	Experiment	KHF	cQRPA	QRPA		Shell Model	
	βdn-decay		(GT)	(GT)	(GT+ff)	OXBASH	ANTOINE
		[32,33]	[34]	[16]	[18]	[31]	[30]
^{129g}Ag	46(7) [14]	100	230	43	42	68	35
^{129m}Ag	158(60) [14]			1230	500	89	40
^{130}Ag	35(10 [35]	29	78	28	25	63	
^{129g}Cd	242(8) [35]	141	385	770	515	180	
^{129m}Cd	104(6) [35]			579	412	229	
^{130}Cd	162(7) [9,36]	147	488	290	241	180	146
^{131}Cd	68(3) [36]	40	207	164	112	94	
^{132}Cd	95(10) [36]	38	191	224	124	82	
^{133}Cd	57(10) [35]	37	157	297	139		
^{133}In	165(3) [37]	41	245	77	62	162	
^{134}In	141(5) [37]	35	190	110	82		
^{135}In	92(10) [37]	34	251	84	63		
^{135}Sn	525(25) [38]	210	5337	8207	1833		
^{136}Sn	250(30) [38]	143	7041	930	543		
^{137}Sn	185(35) [38]	126	2442	1563	706		
^{138}Sn	150(60) [38]	142	3106	234	198		

nuclear properties of far-unstable isotopes are derived when no data are available. As can be inferred from the above discussion, predictions of existing global nuclear models obviously differ considerably when approaching the limits of particle binding. The reason may well be that the model parameters used so far, which were mainly determined to reproduce known properties near β-stability, need not always be proper to be used at the drip-lines. Therefore, experiments very far from stability will be essential to verify possible nuclear-structure changes with isospin, and to motivate improvements in microscopic nuclear theories. It originated, for example, from systematic studies of the evolution of shell structure with increasing distance from stability in the $A \simeq 100$ mass region, that already more than a decade ago Kratz *et al.* concluded that *"the calculated r-abundance "hole" in the $A \simeq 120$ region ... reflects ... the weakening of the shell strength ... below ^{132}Sn$_{82}$."* [13]. This was —in fact— the main motivation for a series of detailed spectroscopic investigations since the late 1980s at CERN/ISOLDE in the ^{132}Sn region (for a recent review, see, *e.g.*, [14]). These studies have largely benefitted from increasing selectivity in the production, separation and detection of isotopically pure beams by applying combinations of a "neutron converter", laser ion sources, isobaric mass separation and multi-parameter detection techniques.

Presently, experimental masses of only 9 r-process "waiting-point" nuclei —two at $A \simeq 80$ and seven in the $A \simeq 130$ region— are known [26]. The situation concerning the gross β-decay properties, $T_{1/2}$ and P_n values, is somewhat better, since they have been determined experimentally for about 35 isotopes in the r-process boulevard, the majority of them lying in and just beyond the $A \simeq 130$ $N_{r,\odot}$ peak [33,26]. Table 1 summarizes our recent $T_{1/2}$ results obtained at CERN/ISOLDE, in comparison with different model predictions [18,30,31,32,33,34]. The measurements were performed by β-neutron coincidence spectroscopy using the high efficiency Mainz neutron longcounter. This 4π detector consists of 64 ^{3}He proportional counters arranged in three concentric rings in a polyethylene matrix. For all these isotopes in the ^{132}Sn region, the energy position and strength (log(ft) value) of the $\nu g_{7/2} \Rightarrow \pi g_{9/2}$ transition dominates the Gamow-Teller (GT) part of the β-decay half-life. For a detailed discussion, see, *e.g.*, [36,38]. As an example for the quality of data that can be obtained for the most exotic nuclei, we show in fig. 1 the β-delayed neutron (βdn) decay curve of the heaviest Cd isotope identified so far, *i.e.* $N = 85$ ^{133}Cd with a $T_{1/2} = 57(10)$ ms [35]. With a P_n value close

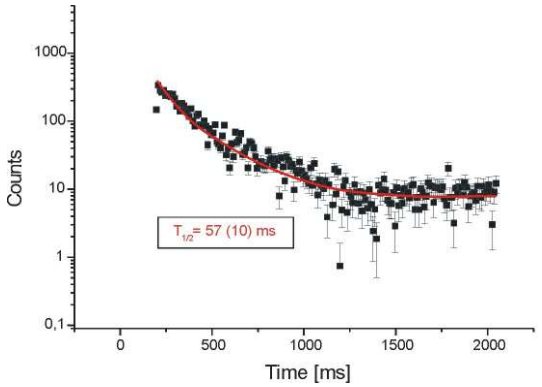

Fig. 1. Delayed neutron spectrum of ^{133}Cd with a half-life of $T_{1/2} = 57(10)$ ms. The longer-lived component is mainly due to the βdn-daughter ^{132}In with $T_{1/2} = 206(5)$ ms.

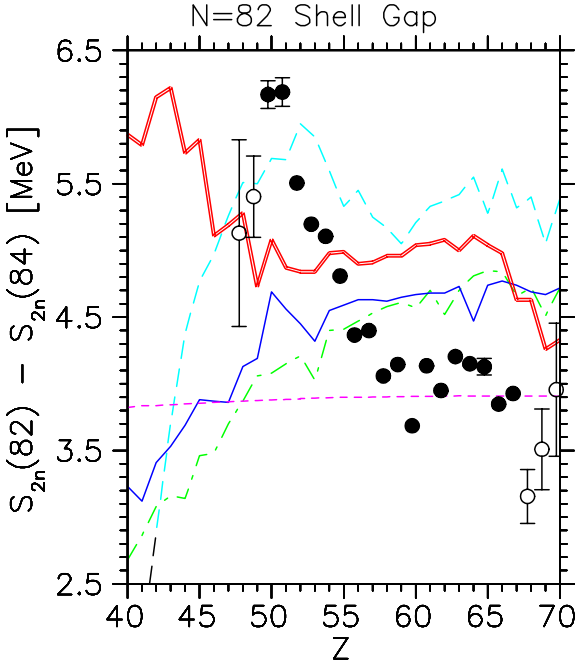

Fig. 2. (Colour on-line) The $N = 82$ shell gap as a function of Z. Theoretical mass predictions (von Groote, magenta short-dashed line [39]; FRDM, red thick solid line [16]; ETFSI-Q, cyan long-dashed line [19]; HFB-2, green dash-dotted line [20]; HFB-8, blue thin solid line [21]) are compared to experimental values from NUBASE [26]. The data for $Z = 47$, 48 and 68–70 (open circles) were deduced from combinations of mass derivatives of measured and short-range extrapolated values.

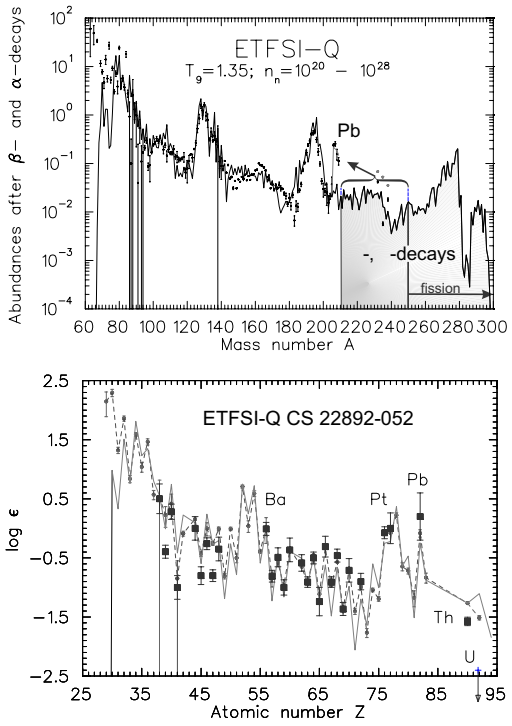

Fig. 3. Upper panel: fit to the isotopic solar r-process abundances (dots; Si = 10^6) obtained from a superposition of sixteen equidistant n_n-components. This result also fits the Pb- and Bi-contributions after summing up the α-decay chains of heavier nuclei. Lower panel: observed neutron-capture elemental abundances in the ultra-metal-poor halo star CS 22892-052 (squares) compared to scaled $N_{r,\odot}$-values (dots) and the calculated r-abundance (full line). The arrow at $Z = 92$ denotes the upper limit of the U abundance.

to 100%, ^{133}Cd mainly decays to $(A-1)$ 206 ms ^{132}In and further "down" to stable ^{132}Xe.

It has been mentioned by several speakers at this conference, that one of the recent experimental highlights in nuclear spectroscopy far from stability with clear astrophysical relevance has been the full spectroscopic study of $N = 82$ ^{130}Cd β-decay [40]. At least for the high-entropy wind scenario of core-collaps SNII explosions —where an r-process starts from a neutron-rich $A \simeq 90$ seed composition beyond $N = 50$— ^{130}Cd is probably *the* most important neutron-magic "waiting-point" isotope. It determines to a large extent the bottle-neck behavior of the r-process matter flow through the respective $A \simeq 130$ $N_{r,\odot}$ peak. In addition to earlier "surprises" in this mass region, indicating that the shell structure around double-magic ^{132}Sn is not yet fully understood [14], also the β-decay of ^{130}Cd (just lying one proton-pair below ^{132}Sn) showed several *a priori* unexpected features. Firstly, although parameter fine-tuned to ^{132}Sn, none of the recent large-scale shell model calculations [29,30,31] was able to correctly *predict* the rather high energy for the main GT-transition to the $\nu g_{7/2} \otimes \pi g_{9/2}$ two–quasi-particle 1^+ level. Secondly, the experiment clearly indicated that the low-lying ff-strength cannot be neglected. The third and probably most important result of this study with both significant nuclear-structure and astrophysics consequences was the fact that the measured Q_β value of 8.34 MeV (which represents the isobaric mass difference between ^{130}Cd and ^{130}In) was considerably higher than the predictions from most global mass models. As is shown in fig. 3 of [40], only some of the more recent models, which explicitly include a *"quenching"* of the $N = 82$ shell gap below ^{132}Sn, were able to roughly reproduce the correct trend of mass differences relative to the "unquenched" FRDM in the Cd isotopic chain. However, beyond ^{130}Cd the predictions of even these models diverge drastically. In order to further illustrate the present situation of mass predictions at the $N = 82$ shell closure, we show here in fig. 2 a comparison of the experimental shell gap (expressed as the energy difference of the two-neutron separation energies (S_{2n}) at $N = 82$ and $N = 84$) as a function of atomic number Z with several mass model predictions. All experimental data were taken from the recent mass evaluation of Audi *et al.* [26]. It should be noted, however, that the S_{2n} values for $Z = 47$, 48 and 68–70 are no "true" experimental values, but combinations of mass derivates from two measurements and one short-range extrapolation, each. These data (open circles) therefore have the largest uncertainties.

It is immediately evident from this figure that *none* of the mass models is able to reproduce the overall experimental trend and in particular the reduction of the shell gap on both sides of the double-magic ^{132}Sn nucleus. The picture also shows that for the $N = 82$ shell closure (as

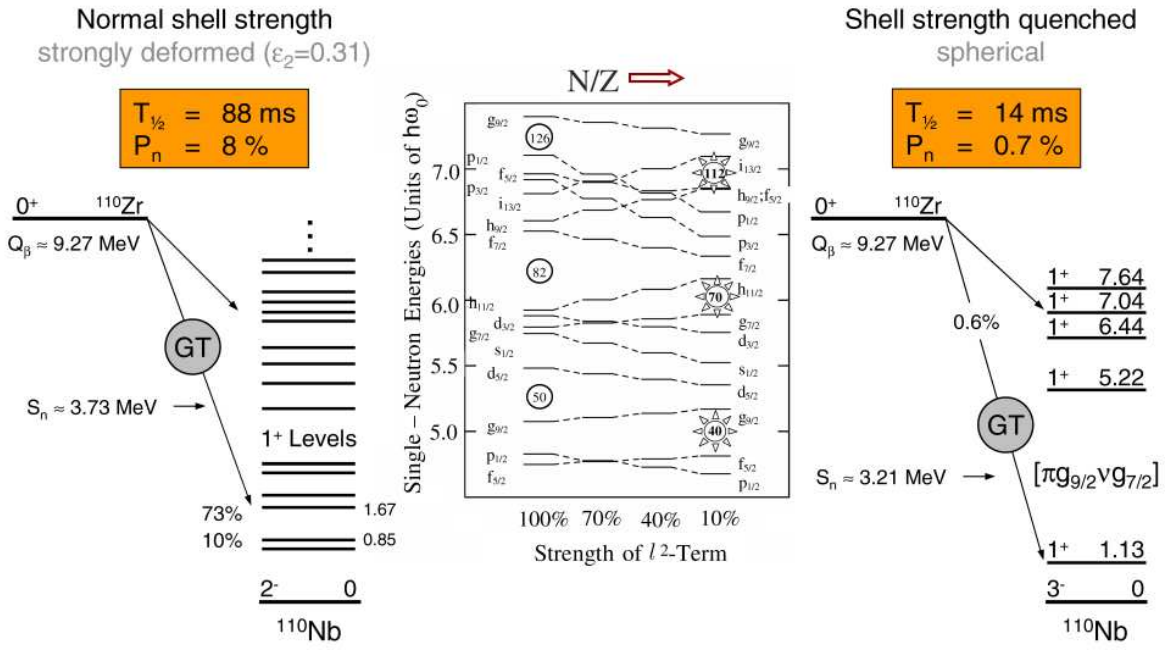

Fig. 4. Possible β-decay properties ^{110}Zr. The left part shows our QRPA predictions for GT-decay of a strongly deformed ^{110}Zr-^{110}Nb system, as expected from the "unquenched" FRDM with the classical neutron shell gaps [17]. The right part shows the GT-decay when assuming ^{110}Zr to be a spherical, doubly semi-magic nucleus with "quenched" shells [41]. In the middle part of the figure, the SP-energies for neutrons in a "classical" Nilsson potential (left part) and in a well where the l^2-term (the parameter μ_n) is reduced gradually to one-tenth of the standard value (right part).

also for $N = 50$ and $N = 126$), there is no improvement of the recent HFB mass model versions of the Montreal-Brussels group over earlier global models. With respect to astrophysical calculations of the $A \simeq 130$ $N_{r,\odot}$ peak, the region from $Z = 50$ down to $Z = 40$ is of particular interest. Here, the ETFSI-Q mass formula [19], which —according to a recent statement of its main author [24]— should be replaced by the new Skyrme HFB models, still provides the "best" trend. In any case, the astrophysical consequence is clear: without the experimental masses (and in particular the crucial Q_β measurement of $N = 82$ ^{130}Cd) together with the corresponding short-range extrapolations of Audi *et al.* [26], any realistic astrophysical calculation of the $120 \leq A \leq 130$ r-abundances would yield unreliable results for the r-proces matter flow at the rising wing of the 2$^{\rm nd}$ $N_{r,\odot}$ peak. It has been shown that this also has considerable consequences for the build-up of the heavier r-elements up to the 3$^{\rm rd}$ peak at $A \simeq 195$ (see, *e.g.*, fig. 8 in [14], or fig. 13 in [7], where the $N_{r,calc}$ fits for the "unquenched" ETFSI-1 [42] and the "quenched" ETFSI-Q are compared). Moreover, as indicated by the calculated Pb and Bi abundances, the "memory effects" from the $N = 82$ and $N = 126$ shell closures will also influence the nucleosynthesis predictions of the Th, U cosmochronometers in ultra-metal-poor halo stars (see, *e.g.*, [7, 43, 44]). As an example, fig. 3 displays our fit to the *isotopic* $N_{r,\odot}$ yields (upper panel) and their conversion to *elemental* abundances (lower panel). There is good agreement between observations and our calculations beyond Ba for the so far best studied halo star CS22892-052.

4 Summary and outlook

In summary, we have reviewed the present status of experimental and theoretical nuclear data for the astrophysical r-process in the ^{132}Sn region. On the experimental side, the results of a detailed spectroscopic study of the decay of the neutron-magic waiting-point isotope ^{130}Cd, as presented in [40], has provided a first *direct* measure for the reduction of the $N = 82$ shell gap by about 1 MeV relative to the double-magic ^{132}Sn. This confirms our earlier predictions of "shell-quenching" in this region, derived from *indirect* experimental indications (see, *e.g.*, [7, 13, 14], and references therein).

On the theoretical side, apart from further fine-tuning of established macroscopic-microscopic models, large-scale microscopic shell-model and HFB approaches with improved predictive power will have to be extended towards *global* applicability in nucleosynthesis calculations. With respect to experiments, in particular further data on the quenching of the classical shells far from stability is needed. In this context, detailed spectroscopic studies of r-process "key isotopes" are inevitable for testing the physical reliablity of any theoretical prediction of gross nuclear properties, which often allow only a limited insight into the underlying nuclear structure.

When accepting the general occurrance of "shell-quenching" far from stability (see, *e.g.* fig. 1 in [41], and middle part of fig. 4), new nuclear structure effects may develop which should already be visible for r-process isotopes. As an example, we show on the left and right side

of fig. 4 possible changes in the decay properties of ^{110}Zr. According to present model predictions (*e.g.*, the "unquenched" FRDM [17]), this nucleus is strongly deformed in its ground state. Hence, the deformed QRPA [18] predicts GT-decay to a multitude of narrow-spaced 1^+ levels in the deformed daughter ^{110}Nb, with the strongest GT-branch to a level at about 1.67 MeV. This decay pattern results in a $T_{1/2} \simeq 88$ ms and a $P_n \simeq 8\%$. When assuming a strongly "quenched" $N = 82$ shell for $Z = 40$, ^{110}Zr will be much less deformed and probably may even become a (near-)spherical, doubly semi-magic nucleus. In this case, the corresponding GT-decay pattern would change drastically, and the resulting gross β-decay properties would be completely dominated by a single allowed transition to a 1^+ state at about 1.13 MeV in ^{110}Nb. The $T_{1/2}$ would become shorter by about a factor 6, and the P_n value would be smaller by about a factor 10. Such differences in both gross β-decay properties should "easily" be detectable, *e.g.* by the measurement of β-delayed neutron emission, provided that ^{110}Zr can be produced at RIB facilitities with sufficient yields, *e.g.* at GSI or MSU by projectile fragmentation. It should be noted in this context, that our basic ideas about an a priori unexpected ground-state structure of a doubly semi-magic ^{110}Zr nucleus may find some support from a completely different mean-field shell model approach, *i.e.* the recent predictions of *"large shell gaps for tetrahedral shapes (pyramid-like nuclei with 'rounded edges and corners')"*, among others, also for nucleon numbers $Z = N = 40$ and $Z = N = 70$ (see, *e.g.*, [45]). These authors calculate the total energy surfaces for neutron-rich $A \simeq 110$ Zr isotopes with low-lying, coexisting tetrahedral, spherical and quadrupole deformed shapes. If our QRPA predictions for the two possible GT-decay patterns shown in fig. 4 are of any guidance, then also the β-decay of a tetrahedral system should contain strong spherical components. In any case, as far as possible astrophysical consequences are concerned, a doubly semi-magic isotope ^{110}Zr would replace the classical $N = 82$ neutron-magic isotope ^{122}Zr as an r-process waiting point. With this, the r-process would enter the $N = 82$ shell at somewhat higher Z than predicted by the "unquenched" mass models, thus helping to avoid the unrealistic r-abundance trough prior to the $A \simeq 130$ $N_{r,\odot}$ peak.

In conclusion, given the close and successful interaction between nuclear physics, cosmo-chemistry, astronomy and astrophysical modelling of explosive scenarios, there is hope to finally solve the problem of the "origin of the heavy elements between Fe and Th, U", which has recently been considered number three of *"The Eleven Greatest Unanswered Questions in Physics"* [46].

We would like to acknowledge discussions with many colleagues about various aspects of nuclear structure and astrophysics, in particular P. Möller, W.B. Walters, J.J. Cowan, B.A. Brown and J.R. Stone. We also thank H.L. Ravn, V. Fedoseyev and U. Köster for their continuous interest and help in improving the target–ionsource conditions at CERN/ISOLDE. Support for this work was provided DFG (grant KR 806/13-1), GSI (grant MZ/KLK) and the HGF (grant VH-VI-061).

References

1. E.M. Burbidge *et al.*, Rev. Mod. Phys. **29**, 547 (1957).
2. A.G.W. Cameron, Atomic Energy of Canada, Ltd., CRL-**41** (1957).
3. C.D. Coryell, J. Chem. Educ. **38**, 67 (1961).
4. W. Hillebrandt, Space Sci. Rev. **21**, 639 (1978).
5. J.J. Cowan *et al.*, Phys. Rep. **208**, 267 (1991).
6. G. Wallerstein *et al.*, Rev. Mod. Phys. **69**, 995 (1997).
7. B. Pfeiffer *et al.*, Nucl. Phys. A **693**, 282 (2001).
8. F.-K. Thielemann *et al.*, Nucl. Phys. A **570**, 329c (1994).
9. K.-L. Kratz *et al.*, Z. Phys. A **325**, 489 (1986).
10. E. Lund *et al.*, Phys. Scr. **34**, 614 (1986).
11. R.L. Gill *et al.*, Phys. Rev. Lett. **56**, 1874 (1986).
12. K.-L. Kratz, Rev. Mod. Astron. **1**, 184 (1988).
13. K.-L. Kratz *et al.*, Ap. J. **402**, 216 (1993).
14. K.-L. Kratz *et al.*, Hyperfine Interact. **129**, 185 (2000).
15. K.-L. Kratz *et al.*, in *Proceedings of the International Conference on Nuclear Data for Science and Technology, ND2004, Santa Fe, New Mexico (USA), 26 September-1 October 2004*, edited by R.C. Haight *et al.*, AIP Conf. Proc. **769**, 1356 (2005).
16. P. Möller *et al.*, At. Data Nucl. Data Tables **66**, 131 (1997).
17. P. Möller *et al.*, At. Data Nucl. Data Tables **59**, 185 (1995).
18. P. Möller *et al.*, Phys. Rev. C **67**, 055802 (2003).
19. J.M. Pearson *et al.*, Phys. Lett. B **387**, 455 (1996) and references therein.
20. S. Goriely *et al.*, At. Data Nucl. Data Tables **77**, 311 (2001).
21. M. Samyn *et al.*, Phys. Rev. C **70**, 044309 (2004), and references therein.
22. D. Lunney *et al.*, Rev. Mod. Phys. **75**, 1021 (2003).
23. Y.-Z. Qian *et al.* (Editors), *Proceedings of the 1st RIA Workshop, The r-Process: The Astrophysical Origin of the Heavy Elements*, *Proceedings from the Institute for Nuclear Theory*, Vol. **13** (World Scientific, 2004).
24. J.M. Pearson in [23], p. 43, and references therein.
25. J. Engel in [23], p. 53, and references therein.
26. G. Audi *et al.*, Nucl. Phys. A **729**, 3 (2003).
27. S. Goriely *et al.*, Nucl. Phys. A **750**, 425 (2005).
28. P. Möller, private communication (2004).
29. T. Nikšič *et al.*, Phys. Rev. C **71**, 014308 (2005).
30. G. Martinez-Pinedo, Nucl. Phys. A **668**, 357c (2000) and references therein.
31. B.A. Brown *et al.*, Nucl. Phys. A **719**, 177c (2003) and references therein.
32. K.-L. Kratz, G. Herrmann, Z. Phys. **263**, 179 (1974).
33. B. Pfeiffer *et al.*, Prog. Nucl. Energy **41**, 39 (2002).
34. I.N. Borzov *et al.*, Phys. Rev. C **62**, 035501 (2000).
35. O. Arndt, Diploma Thesis, University of Mainz (2003).
36. M. Hannawald *et al.*, Phys. Rev. C **62**, 054301 (2000).
37. I. Dillmann *et al.*, Eur. Phys. J. A **13**, 281 (2002).
38. J. Shergur *et al.*, Nucl. Phys. A **682**, 493 (2001).
39. H. von Groote *et al.*, At. Data Nucl. Data Tables **17**, 418 (1976).
40. I. Dillmann *et al.*, Phys. Rev. Lett. **91**, 162503 (2003).
41. B. Pfeiffer *et al.*, Acta Phys. Pol. B **27**, 475 (1996).
42. Y. Aboussir *et al.*, At. Data Nucl. Data Tables **61**, 127 (1995).
43. K.-L. Kratz *et al.*, New Astr. Rev. **48**, 109 (2004).
44. J.J. Cowan *et al.*, Ap. J. **521**, 194 (1999).
45. J. Dudek *et al.*, Phys. Rev. Lett. **88**, 252502 (2002), and Phys. Rev. C **69**, 061305 (2004).
46. E. Haseltine, Discover Mag. **23**, No. 2 (2002).